Research Article

Novel green synthesis of silver nanoparticles using clammy cherry (*Cordia obliqua Willd*) fruit extract and investigation on its catalytic and antimicrobial properties

Femina Kanjirathamthadathil Saidu[1,2] · Anjaly Mathew[3] · Asna Parveen[2] · Vijeesh Valiyathra[3] · George Vazhathara Thomas[1]

Abstract

In this study, highly monodispersed, exceptionally stable, spherical silver nanoparticles (AgNPs) were successfully synthesized by the microwave assisted rapid and cost-effective green method. Aqueous extract of clammy cherry (*Cordia obliqua Willd*) fruit was used as the green reductant, and capping agent for the synthesis of AgNPs and the effect of different synthesis parameters on the optical properties of the synthesized AgNPs was also studied. The characterization of synthesized AgNPs by Fourier transform infrared spectroscopy, X-ray diffraction studies, UV–visible spectroscopy, scanning electron microscopy and transmission electron microscopy (TEM) revealed the formation of small AgNPs with narrow size distribution. TEM studies corroborated that the AgNPs are highly crystalline and spherical with an average diameter of 7.13 nm. The cyclic voltammetry profile of AgNPs modified electrode in NaOH depicted prominent redox peaks evidencing an impressive electrochemical response. The AgNPs manifested high catalytic activity towards reduction of methyl orange and rhodamine blue with apparent rate constant 0.3038 min^{-1} and 0.1542 min^{-1} respectively. Additionally, the prepared AgNPs exhibited strong antibacterial efficacy against the tested microbes.

Electronic supplementary material The online version of this article (https://doi.org/10.1007/s42452-019-1302-x) contains supplementary material, which is available to authorized users.

✉ George Vazhathara Thomas, georgevtsjc@gmail.com | [1]Department of Chemistry, St. Joseph's College, Moolamattam, Idukki, Kerala 685591, India. [2]Department of Chemistry, Maharaja's College, Ernakulam, Kerala 682011, India. [3]Department of Chemistry, Sree Neelakanta Govt. Sanskrit College, Pattambi, Palakkad, Kerala 679306, India.

SN Applied Sciences (2019) 1:1368 | https://doi.org/10.1007/s42452-019-1302-x

Received: 13 June 2019 / Accepted: 18 September 2019 / Published online: 10 October 2019

Graphic abstract Green synthesis of silver nanoparticles using clammy cherry fruit extract

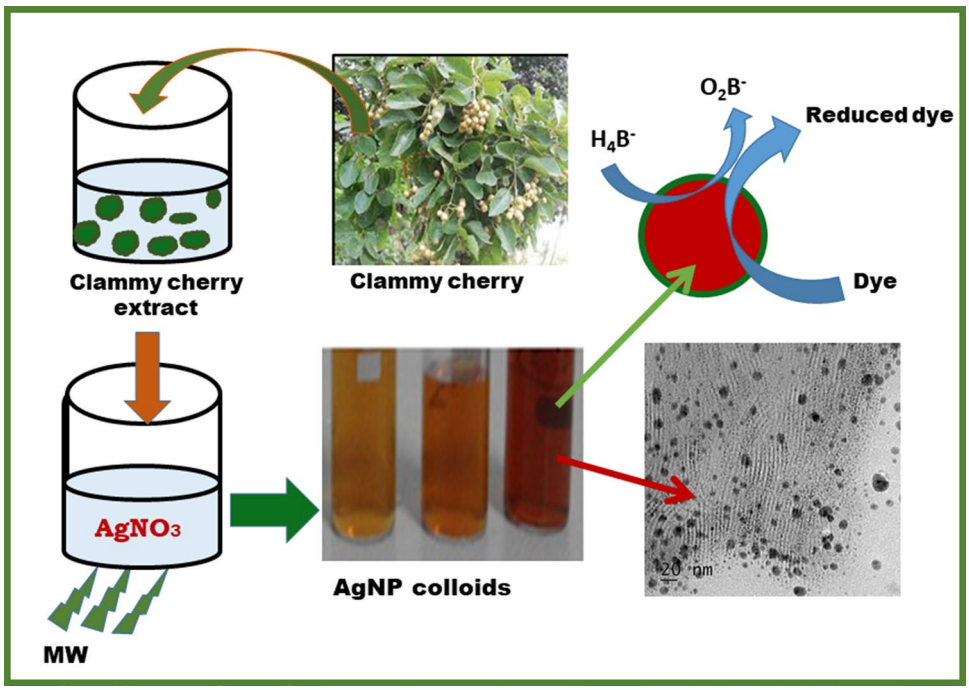

Keywords Silver nanoparticles · Microwave · Green · Reduction · Catalysis · Surface plasmon resonance · Methyl orange · Rhodamine blue

1 Introduction

Nanotechnology is a fast developing research field making its impact on all spheres of human life. Currently, the synthesis of noble metal nanoparticles has drawn considerable attention by nanochemists because of their exceptional physio-chemical characteristics and their wide biomedical, sensing and catalytic applications [1–5]. Silver nanoparticles (AgNPs) are extensively studied compared to nanoparticles of Au, Pt, and Pd because of its ease of synthesis and lower cost. AgNPs shows excellent optical, electronic, antimicrobial and catalytic properties [6–8]. Versatile organic transformations for the production of industrially and therapeutically important organic molecules have been successfully carried out with high efficiency and selectivity using nanosilver based catalytic systems [9–11]. The catalytic activity of metal nanoparticles has extensively investigated in the field of water pollution remediation. Many research groups have demonstrated the effective utilization of noble metal NPs or metal NP incorporated composites systems as a suitable redox catalyst for the degradation of various organic pollutants like dyes, drugs and aromatic nitro compounds [12–19]. Additionally unique electrochemical features and high conductivity of AgNPs identifies AgNPs as a good candidate for selective and sensitive monitoring of biomolecules and pharmaceuticals [20–22]. Earlier reports have shown that size, shape, and surface features are critical in deciding performance of their so far mentioned catalytic and sensing applications [21–25]. It is reported that the cytotoxicity of AgNPs against diseases like HIV and cancer are also size dependent [2, 26, 27]. In this context, the method of synthesis, especially the nature of stabilizing agents, reducing agent and other synthesis parameters have a critical role in deciding the properties of the AgNPs.

Due to the potential applications in diverse fields, there is a constant urge for the development of the fast synthesis of AgNPs with controllable size and uniqueness in good yield. To date, a number of chemical reduction procedures have been reported for the synthesis of AgNPs [7, 28]. Even if this synthetic route allows the fast synthesis of AgNPs in bulk scale, most of the reagents used as reducing and/stabilizing agents are toxic and not biocompatible. Hence the AgNPs obtained by such chemical routes cannot be used for the biomedical application, such as drug carrier and or in vivo imaging studies.

Recently, the biosynthesis of metal nanoparticles (MNPs) have been proposed as a cost-effective and eco-friendly substitute to chemical methods. Many studies have been demonstrated the biosynthesis of AgNPs mediated by the

microorganism or by phytochemicals or enzymatic synthesis [11, 18, 19, 29–33]. Among the biological methods, photosynthesis which involves reduction by phytochemicals derived from plants seems to be the superior choice. Phytochemical mediated synthesis is considered as a green alternative as it utilizes nontoxic, green reducing and stabilizing agent, thus making the method simple, economical environment-friendly and biocompatible. However, synthesis of AgNPs by the phytochemical reduction methods are rather slow compared to conventional chemical reduction and it was considered as the major limitation that faced during the earlier periods of green synthesis. Currently, by coupling plant-mediated synthesis with microwave (MW) assisted synthetic techniques, the biosynthesis can be conveniently carried out rapidly with good yield [4, 34, 35]. MW assisted chemical transformations a simple yet versatile eco-friendly process to achieve the fast synthesis of metal NPs.

Here, we investigated the role of fruit extract of *Cordia obliqua Willd* as the green reductant and stabilizing agent during the formation of AgNPs *Cordia obliqua Willd* commonly known as clammy cherry is a plant that belongs to Boraginaceae family which has widely distributed warmer regions of India and Ceylon [36, 37]. Traditionally the plant is of great medicinal value. The phytochemical screening studies on clammy cherry extract reported earlier revealed the presence of numerous poly-functional molecules like carbohydrates, proteins, amino acids, flavonoids, phenolic compounds, alkaloids, glycosides and sugar in different part of the plant [36, 37].

We have demonstrated the ability of this clammy cherry derived phytochemicals as reducing and capping agent during the formation of AgNPs. In the present work, we could synthesize spherical AgNPs with narrow size distribution under microwave irradiation of few minutes. The use of water for extraction and reaction medium is a further add-on to the green chemistry policy. The effect of the MW power, irradiation time, and concentration of silver nitrate solution on AgNPs characteristics was also investigated. Impressive electrochemical response and high catalytic activity towards the reduction of organic dyes are highly promising for its futuristic applications in diverse fields including catalysis and sensing. This study has established a rapid, cost-effective and eco-friendly procedure for the synthesis of highly stable AgNPs having hopeful application potentials.

2 Experimental

2.1 Materials and methods

The chemicals, silver nitrate ($AgNO_3$), sodium borohydride ($NaBH_4$), graphite powder, paraffin liquid and sodium hydroxide used in the study were purchased from Merck Chemicals Ltd, Mumbai, India. The organic dyes methyl orange (MO) and rhodamine blue (RhB) have purchased from Nice Chemicals, India. Microwave oven [wave (LG) Model 1S2021CW at 2450 MHz] was used for the AgNPs synthesis.

2.2 Preparation of clammy cherry extract

Ripened clammy cherry fruits were collected from the Maharajas college campus, Kerala, India. 10 g of fruit was washed thoroughly with deionized water several times, then peel was removed, and the pulp along with seed was refluxed with 100 mL water under microwave heating for 2 min at 350 W. The aqueous extract is cooled, filtered with Whatmann 40 filter paper and filtrate is used for synthesis.

2.3 Synthesis of silver nanoparticles (AgNPs)

Silver NPs was prepared by heating a solution of $AgNO_3$, and clammy cherry extract in a domestic MW oven. In a typical procedure, 10 mL of the clammy cherry extract (10 g/100 mL) was mixed well with 20 mL of 1 mM $AgNO_3$ solution and irradiated in MW oven at 2.45 GHz under 350 W for about 8 min. Wherein, the color of the solution changes to light yellowish to reddish brown indicating the formation of the AgNPs. The effect of different parameters such as MW power, the period of exposure, the concentration of $AgNO_3$ and composition of clammy cherry extract were also investigated. The entire process was monitored by recording the UV–Vis spectrum using the reaction mixture collected at regular intervals.

2.4 Characterization

Thermoscientific evolution 160 UV–VIS Spectrometer is used for recording the UV–Vis spectrum of the periodically collected reaction mixtures. The surface morphology of AgNPs was analyzed by scanning electron microscope (SEM) using VEGA3 TESCAN. Transmission electron microscopic images were done using a JEOL JEM-2100 microscope. X-ray diffraction (XRD) studies were carried out using powdered AgNPs which are collected by ultracentrifugation followed by drying in a vacuum oven for 24 h. Fourier transform infrared spectroscopy (FTIR) spectra of the vacuum dried clammy cherry extract and AgNPs were recorded in the range 4000–450 cm^{-1} using Perkin Elmer FTIR spectrometer.

2.5 Antibacterial assay

Biological studies were conducted for determining the bactericidal activity of synthesized AgNPs against four

human pathogenic bacteria namely *Escherichia coli*, *Bacillus circulans*, *Pseudomonas aeruginosa*, and *Staphylococcus aureus*. Mueller–Hinton agar (MHA) well diffusion method was employed to investigate the antibacterial activity of clammy cherry stabilized silver NPs. 25 µL spore suspension (10–100 spore/mL) of *S. aureus*, *E. coli*, *B. circulans*, *P. aeruginosa* were added to a sterile Muller Hinton medium fast before solidification, then poured into sterile Petri dishes (9 cm in diameter) and spread using a cotton swab. Sterilized disc (6 mm) is taken, and 10 µL of nanoparticles solution was dropped into it and was kept in the Petri dish. Sealed the Petri dish with cling film and incubated for 16 h. Inhibition zones were detected around the disc and measured.

Minimum inhibitory concentration (MIC) is the lowest concentration of a chemical which prevents visible growth of a bacterium. MIC was determined by resazurin based microtiter dilution assay (RMDA) method. In a standard procedure, RMDA was done using, 96 well microtiter plates (HiMedia) under sterile conditions. The first row of the plate is filled with 100 µL of AgNPs (1 mg/mL) dissolved in sterilized water. All the wells of microtiter plates are packed with 50 µL of Luria broth. By transferring 50 µL AgNPs solution from the first row to the next wells in the next row of the same column, a two-fold serial dilution is achieved and so that each well has 50 µL of test material in serially descending concentrations. 2 µL of resazurin indicator solution was added into each well to impart purple color. Finally, 10 µL bacterial suspension was added to each well to achieve a concentration of 5×10^6 CFU/mL. Then each plate was covered with cling film to avoid the dehydration of bacterial culture. There was a set of 3 controls for each microtiter plate, a first column with the positive control (Ampicillin), a second column with all reagents but without AgNPs solution and the third column with all solutions along with 10 µL of Luria broth instead of the bacterial solution. The entire plates are incubated at 37 °C for 1 day. Any color change observed from purple was taken as positive. The lowest concentration of the sample at which no color change occurred was recorded as the MIC value. All the experiments are performed in triplicates and average was taken as the MIC of synthesized AgNPs.

2.6 Catalytic activity studies

The catalytic activity of the clammy cherry stabilized AgNPs was evaluated by monitoring the reduction of organic pollutants like methyl orange (MO) and rhodamine blue (RhB) under pseudo-first order condition in presence of relatively high concentration of sodium borohydride. The reaction is monitored by recording the absorption spectra in each min in the range of 200–800 nm at room temperature using Thermo scientific evolution 160 UV–Vis Spectrophotometer.

2.7 Electrochemical studies

The electrochemical response of the AgNPs was studied by cyclic voltammetric (CV). The CV was recorded with AgNPs modified carbon Paste Electrode (CPE) was carried out in Metrohm Auto lab Potentiostat/Galvanostat (Model No. AUT87141) furnished with NOVA 2.1 software. A three-electrode electrochemical setup containing modified carbon paste electrodes as working electrode, Pt wire as a counter electrode and Ag/AgCl reference electrode is used for recording CV. Carbon paste prepared by thorough mixing graphite powder and paraffin oil (weight ratio of 70:30) was packed in a clean glass tube. Silver wire was inserted into carbon paste for electrical contact. The CPE surface was modified by drop casting 10 µL of the AgNPs to get AgNPs/CPE.

3 Result and discussion

3.1 Synthesis of AgNPs and UV–Vis spectral studies

A fast synthetic protocol for the synthesis highly stable AgNPs by exploiting the reducing and stabilizing capabilities of the phytochemicals present in the aqueous extract of the Clammy Cherry was established here. The presence of numerous poly-functional molecules like carbohydrates, proteins, amino acids, flavonoids, phenolic compounds, alkaloids, glycosides and sugar in different part of the clammy cherry have been established in their phytochemical screening studies on clammy cherry reported earlier [36, 37]. The formation of AgNPs was evidenced by the apparent color change of the solution from colorless to dark red within a short period. These biomolecules are considered to be responsible for the fast reduction of silver ions and stabilization of AgNPs. Here the use of water as the solvent for extraction and as the reaction medium was a further add-on to green chemistry policy. Additionally, MW-assisted route has radically reduced the reaction time and increased the yield of AgNPs during the current process. A schematic representation of MW assisted synthesis of AgNPs using clammy cherry extract is depicted in Fig. 1.

As the MW heating of the reaction mixture containing clammy cherry extract and $AgNO_3$ solution proceeds, light yellow color has appeared within few seconds, and the color got intensified on increasing the time of MW exposure as illustrated in Fig. 2.

UV–Vis spectroscopy was used to monitor the progress of AgNPs formation. No absorption peaks are seen for both $AgNO_3$ and clammy cherry extract solution in the visible

Fig. 1 Pictorial representation of MW assisted synthesis of AgNPs using clammy cherry extract

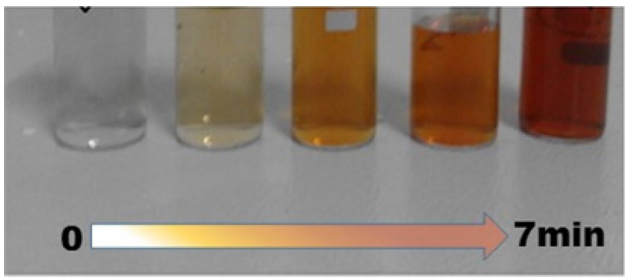

Fig. 2 The visual color change observed during MW exposure of $AgNO_3$ (1 mM) with clammy cherry extract (10 g/L)

region (red and black curve of Fig. 3 respectively), and absorption peaks were observed at 304 nm and 283 nm for $AgNO_3$ and Clammy cherry extract solution respectively. However, after exposing the mixture of two solutions to MW radiation, a typical absorption band with λ_{max} around 409–425 nm corresponding to surface plasmon resonance (SPR) of AgNPs were observed which confirmed the formation of AgNPs having a size between 5 and 20 nm [38].

The stability of prepared AgNPs is a valuable parameter to be analyzed and achieved. Excellent stability and durability of AgNPs are highly appreciated for their sensing and catalytic applications. It is observed that the Clammy cherry reduced AgNPs are stable for more than 6 months without coagulation under refrigeration. The UV–Vis spectra of the AgNPs recorded after 6 months presented in Fig. 3 (blue line) still shows SPR with absorption maxima

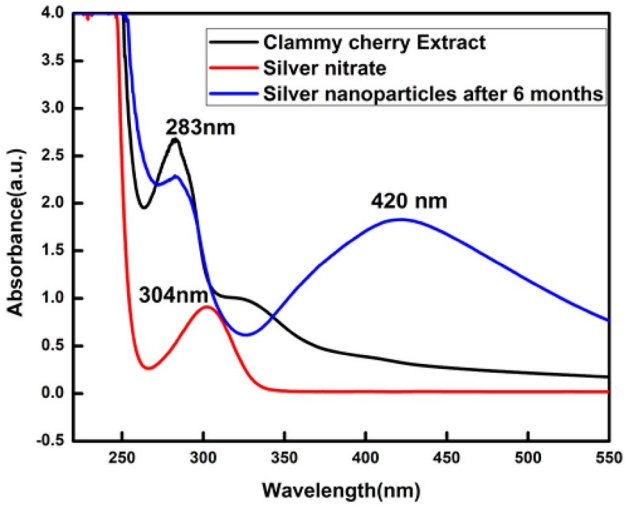

Fig. 3 UV visible spectra of clammy cherry extract (black), silver nitrate solution (red), and AgNPs solution after 6 months (blue)

at 420 nm confirming the existence of highly dispersed AgNPs.

The progress of the bioreduction was followed by UV–Vis spectral studies and the spectra are presented in Fig. 4a–d. Results reveal that rate of formation, size, and optical properties are found to be influenced by the reaction parameters such as the concentration of $AgNO_3$, the composition of extract, MW power and time of exposure. Among the four synthesis parameter investigated, it is clear from spectral studies that like time of exposure, MW power has a profound effect on the nature of AgNPs which is reflected in Fig. 4a. At low MW power as low as 75 W, no color change was observed for 5 min of exposure, while the reduction was much fast at higher MW power. Hence, it is be attributed that minimum activation energy required for the reduction and formation of AgNPs. An increase in the absorption intensity of SPR absorption with the time of MW exposure was observed suggesting more population of AgNPs in the reaction medium due to more reduction (Fig. 4b). After 7 min of MW treatment under 350 W power, the intensity of absorption remains almost the same confirming the complete reduction of silver ion. It is observed that on increasing the time of MW exposure, a slight shift in SPR maxima towards lower wavelength was observed. Figure 4c revealed that even low concentration of extract (10 g/L) is sufficient for the effective reduction and stabilization of AgNPs. From Fig. 4d it is clear that the intensity of absorption and hence population of AgNPs shows a direct dependence with the concentration of $AgNO_3$ solution. At higher $AgNO_3$ concentration coagulation was observed resulting in a black precipitate which is attributed to the fast reduction without proper

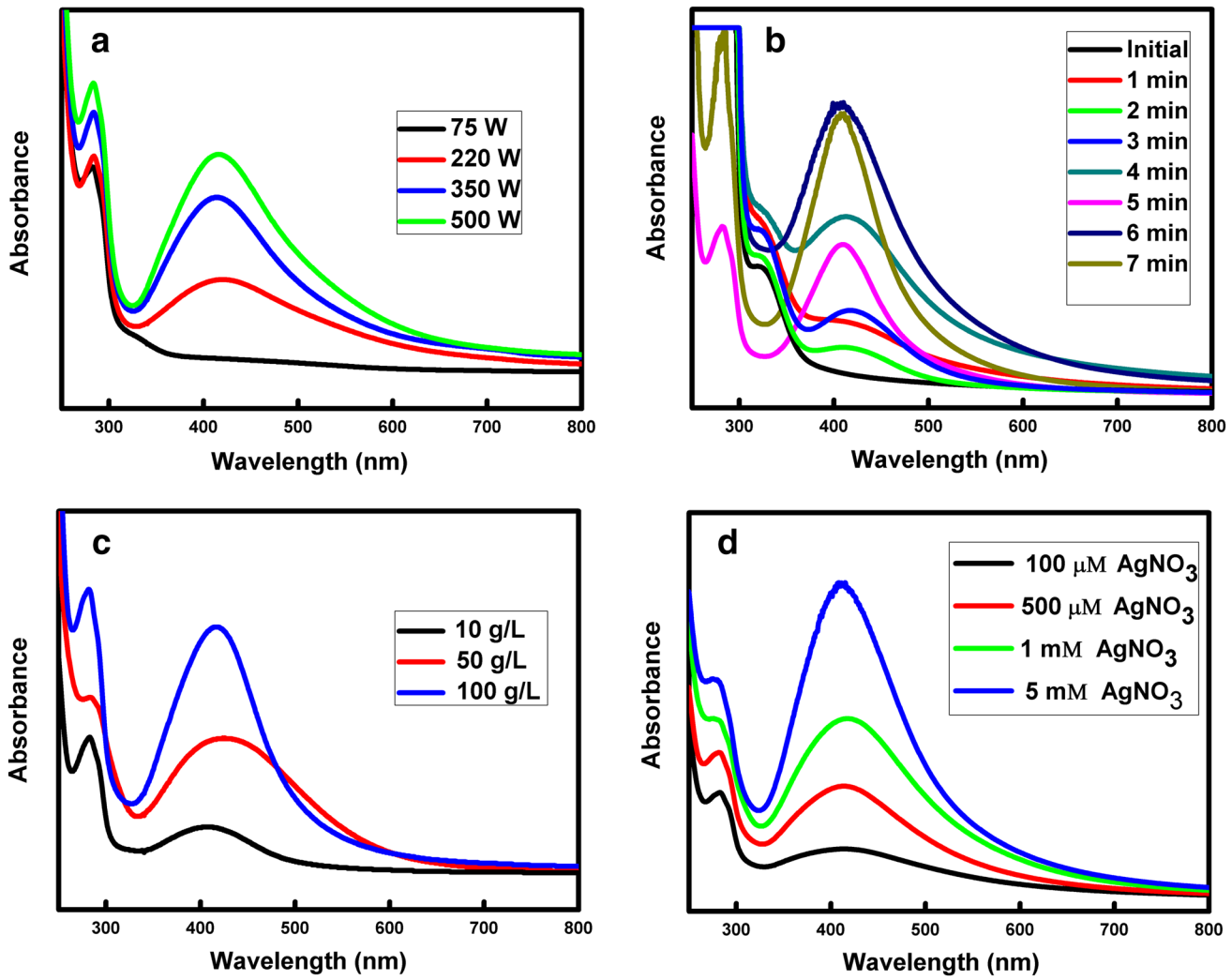

Fig. 4 UV–Vis spectra recorded at different synthesis condition **a** effect of MW power, **b** effect of time of exposure, **c** effect of clammy cherry extract concentration, and **d** effect of concentration $AgNO_3$

passivation. This might be because of the ineffective passivation of AgNPs lesser number of plant metabolites compared to silver ions. Most of the UV–Vis spectra observed were sharp and contains single SPR absorption maxima was indicating the spherical AgNPs are of narrow size distribution. There is no agglomeration since the particles are better stabilized, thus UV–Vis spectral study corroborates the unique capping effect of the phytochemicals present in the clammy cherry extract. The different synthesis conditions adopted and its effect on SPR absorption maxima of corresponding AgNPs formed are summarized in Table S1 (Supporting information).

3.2 FTIR studies

To identify the possible functional groups involved in the reduction and stabilization of the AgNPs, FT-IR spectral studies of the vacuum dried clammy cherry extract and AgNPs were carried out, and it is presented in the Fig. 5 (curve black and red respectively). FTIR spectrum of Clammy cherry extract shows some distinct peaks corresponding to functional groups such as –OH, –NH, –CONH, –COOH, C=O, and C–O–C linkages and aromatic C=C linkages. The broad peak at 3247 cm^{-1} and sharp peak 1575 cm^{-1} are assigned to H-bonded amino/hydroxyl stretching and bending respectively. The peak around 1390 cm^{-1} is assigned to the –COO stretching from amino acid groups. The peak at 1719 cm^{-1} suggests the presence of carboxyl and/kenotic functionalities. Hence it is inferred that Clammy cherry extract contains biomolecule having an active functional group which can reduce silver ion to metallic silver and can take part in stabilizing interaction with AgNPs. Earlier studies have confirmed that carbonyl, ester, amino, hydroxyl, and phenolic groups effectively

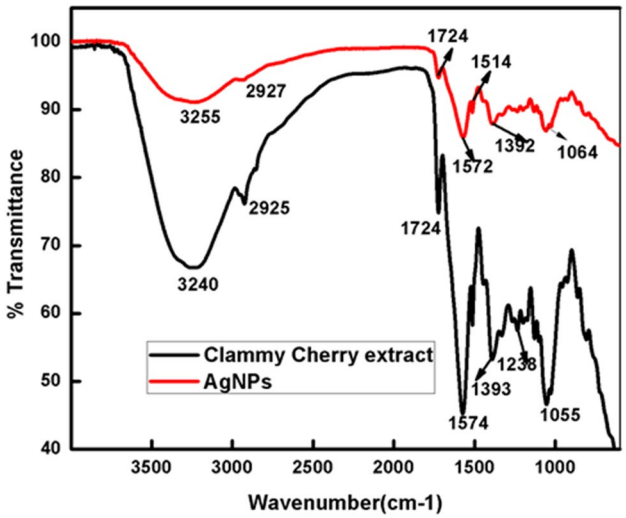

Fig. 5 FTIR spectra of clammy cherry fruit extract and synthesized AgNPs

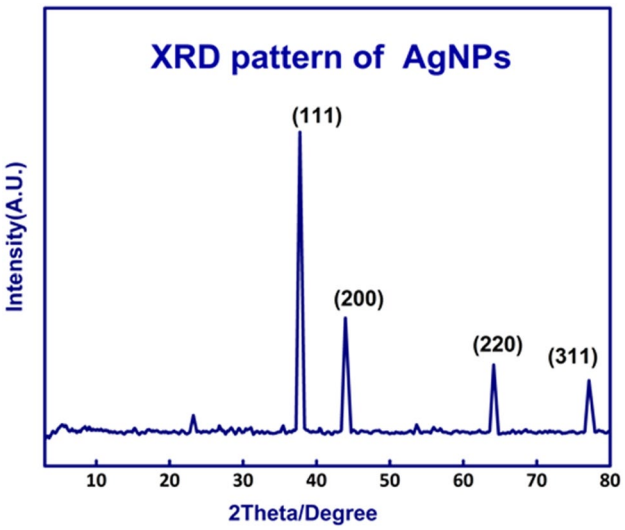

Fig. 6 XRD pattern of the clammy cherry extract reduced AgNPs

bind with the noble metals through their coordinating and polar interactions [4]. In the present study, it is suggested that these identified functional groups may interact with silver and forms a capping layer over the AgNPs which prevents their clustering ensuring proper stabilization. Further, the FTIR spectrum of dried AgNPs showed peaks similar to those of the clammy cherry extract hence it is suggested that AgNPs might be covered with a layer of phytochemicals derived from clammy cherry.

3.3 XRD studies

The XRD pattern observed for the clammy cherry extract reduced AgNPs is presented in the Fig. 6. The XRD spectra show sharp peaks corresponding to the characteristic diffraction from (111), (200), (220), and (311) planes of the *fcc* lattice of metallic silver proving that the prepared AgNPs are highly crystalline (JCPDS: 01-089-3722). No prominent peaks corresponding to silver oxide or any other silver compounds were observed confirming that the AgNPs are composed of pure metallic phase [2].

3.4 SEM analysis

Figure 7 depicts the SEM images clammy cherry stabilized AgNPs. It is observed that the clustered AgNPs forms well-defined spherical microstructures and the aggregated microspheres are coated by a thin film composed of various phytochemicals contained in the mucilage or gum of aqueous extract of clammy cherry. Similar observations were also made during plant-mediated synthesis of the metal nanoparticle by some other research groups [39, 40].

3.5 TEM analysis

The size, morphology and crystal structure of synthesized silver nanoparticles were further studied in detail by transmission electron microscopy (TEM) and the TEM images were shown in Fig. 8a, b. The TEM images, confirms the AgNPs are almost spherical and monodisperse. The small size and narrow size distribution are attributed to the fast reduction under MW irradiation. The particle size distribution was shown in the histogram (Fig. 8d). The average particle size measured from the TEM images is observed to be 7.13 nm. Selected area electron diffraction (SAED) pattern shows concentric rings which reveal the crystalline nature of the synthesized Ag NPs. The particles are well isolated from each other by the capping phytochemicals. Hence no particle aggregation was observed as evident from the TEM image and results confirms the effective capping ability of the clammy cherry derived phytochemicals.

3.6 Cyclic voltammetry studies

The electrochemical response of the AgNPs modified CPE was analyzed by recording CV in 0.1 M NaOH solution, and it was compared with bare CPE. The AgNPs modified electrodes show substantial enhancement in current response compared to unmodified CPE. In the CV curve of the AgNPs/CPE (Fig. 9 red curve), all prominent peaks corresponding to particular redox transitions of metallic silver to silver oxide were observed [8]. The significant current response is due to the large electrochemical surface area which is attributed to the smaller size, large surface to volume ratio and better dispersion of highly conducting AgNPs. The good electrocatalytic

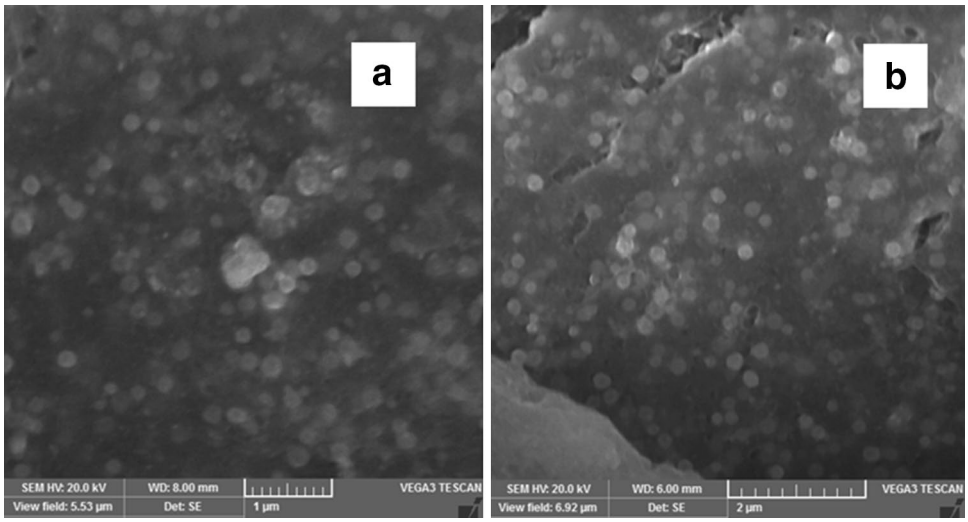

Fig. 7 SEM images of AgNPs under **a** low and **b** high magnification

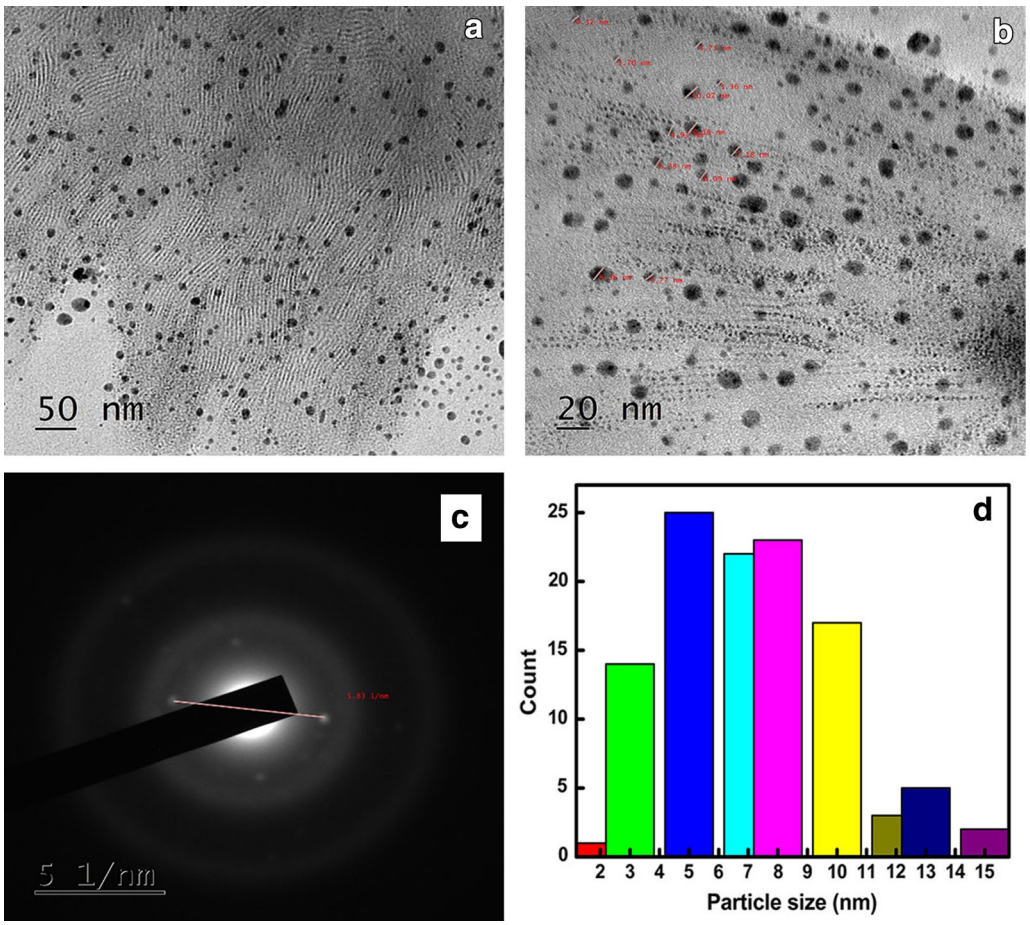

Fig. 8 TEM of Ag NPs under different magnification (**a**, **b**), SAED pattern (**c**) and particle–size histogram (**d**)

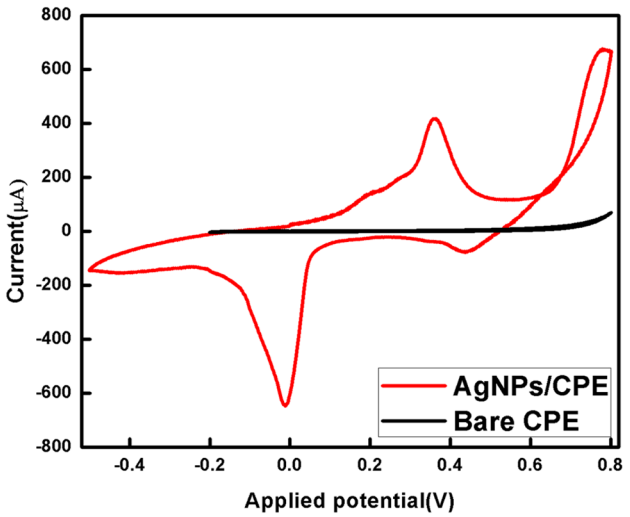

Fig. 9 The CV of AgNPs modified CPE (red curve) and bare CPE (black) recorded in 0.1 M NaOH against Ag/AgCl reference electrode and, Pt as a counter electrode at a scan rate of 50 mV s^{-1}

and sensing performance was anticipated based on the CV results, and studies on electrochemical sensing of biomolecules using synthesized AgNPs are underway.

3.7 Antibacterial studies

In this study, we have investigated the in vitro antibacterial activity of the synthesized Ag NPs against the common pathogenic bacteria both Gram-positive bacteria [*Bacillus circulans* (*B. circulans*), *Staphylococcus aureus* (*S. aureus*)] and Gram-negative bacteria [*Pseudomonas aeruginosa* (*P. aeruginosa*) and *Escherichia coli* (*E. coli*)] using Mueller–Hinton Agar (MHA) well diffusion method. The bacterial strains impregnated with AgNPs were incubated for 24 h in the dark at 37 °C, and the corresponding photographs are shown in Fig. 10. The observation of distinct zones of inhibition around the discs suggests the strong antibacterial activity of the prepared AgNPs. Additionally, the photographs indicate that the extent of antibacterial activity has a direct dependence with the dosage of AgNPs colloid, and zone observed for 20 µL of AgNPs colloid is higher than that corresponds to 10 µL in all cases.

The MIC values AgNPs for each bateria determined by the RMDA methods are shown in Table 1 and the values are found to be significantly lower than that of standard positive control ampicillin, The observed low MIC values again confirm high antibacterial activity of the clammy cherry stabilized AgNPs (photographed image showing results of RMDA is shown in Fig. S1 (supporting information).

Antibacterial activity of silver nanoparticle and silver ions are well known, but still, an exact mechanism of action is not precise. Different research groups have suggested various modes of bacteriostatic action. It is proposed that the bacterial cell death is due to the structural and morphological changes induced by AgNPs. When AgNPs comes in contact with the bacteria, they adhere to the cell wall and cell membrane. Once bound, some of the silver may penetrate through the cell wall and interacts with DNA and RNA and blocks the bacterial cell's replication [2, 4, 29, 41]. Although the proposed mechanism varies for every type of cell, as there is great variation in their cell wall composition, AgNPs with an average size of 10 nm or less shows better interactions that significantly increase their bactericidal

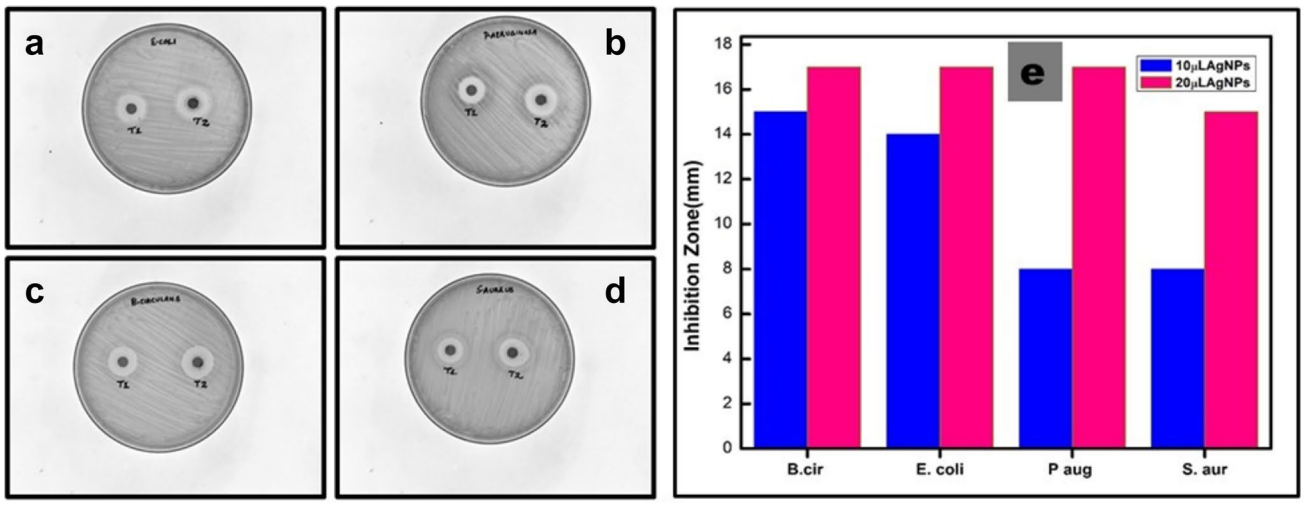

Fig. 10 Photographs showing the zone of inhibition observed for on addition of AgNPs colloid (T1-10 µL and T2-20 µL) against bacterial strains. **a** *Bacillus circulans*, **b** *Escherichia coli*, **c** *Pseudomonas aeruginosa*, **d** *Staphylococcus aureus* and **e** histogram showing the antibacterial activity of AgNPs

Table 1 MIC values of prepared AgNPs obtained from RMDA method

Bacteria	Minimum inhibitory concentration (MIC) (µg/mL)	Standard drug ampicillin (µg/mL)
Pseudomonous aeruginosa	0.0275	3.125
Staphylococcus aureus	0.0551	0.3906
Bacillus circulans	0.0551	25
Escherichia coli	0.1103	0.7812

activity. It has been reported that the size of the particle significant role in antimicrobial activity [26, 29, 42]. The smaller particles can penetrate the cell wall and interact with the cell metabolites quickly. Here the excellent bactericidal activity of as-synthesized AgNPs is attributed to the smaller size and high surface to volume ratio.

3.8 Catalytic studies

The catalytic efficiency of the biosynthesized AgNPs was investigated towards the reductive degradation of rhodamine blue (RhB) and methyl orange (MO) with an excess of sodium borohydride as a reductant in the aqueous medium. The progress of both catalytic processes was followed by recording in situ UV–Vis spectrum at each minute, and the time-dependent UV–Vis spectra are presented in Fig. 11. As time proceeds there is a visually observable color change in the reaction mixture and the solution becomes colorless within 9 min for MO (Fig. 11a) and 14 min for RhB (Fig. 11b). As the reductant concentration was high, the reaction is supposed to proceed under pseudo-first order condition, and the kinetics of the AgNPs catalyzed reduction as studied by noting the absorbance at 464 nm and 554 nm for MO and RhB

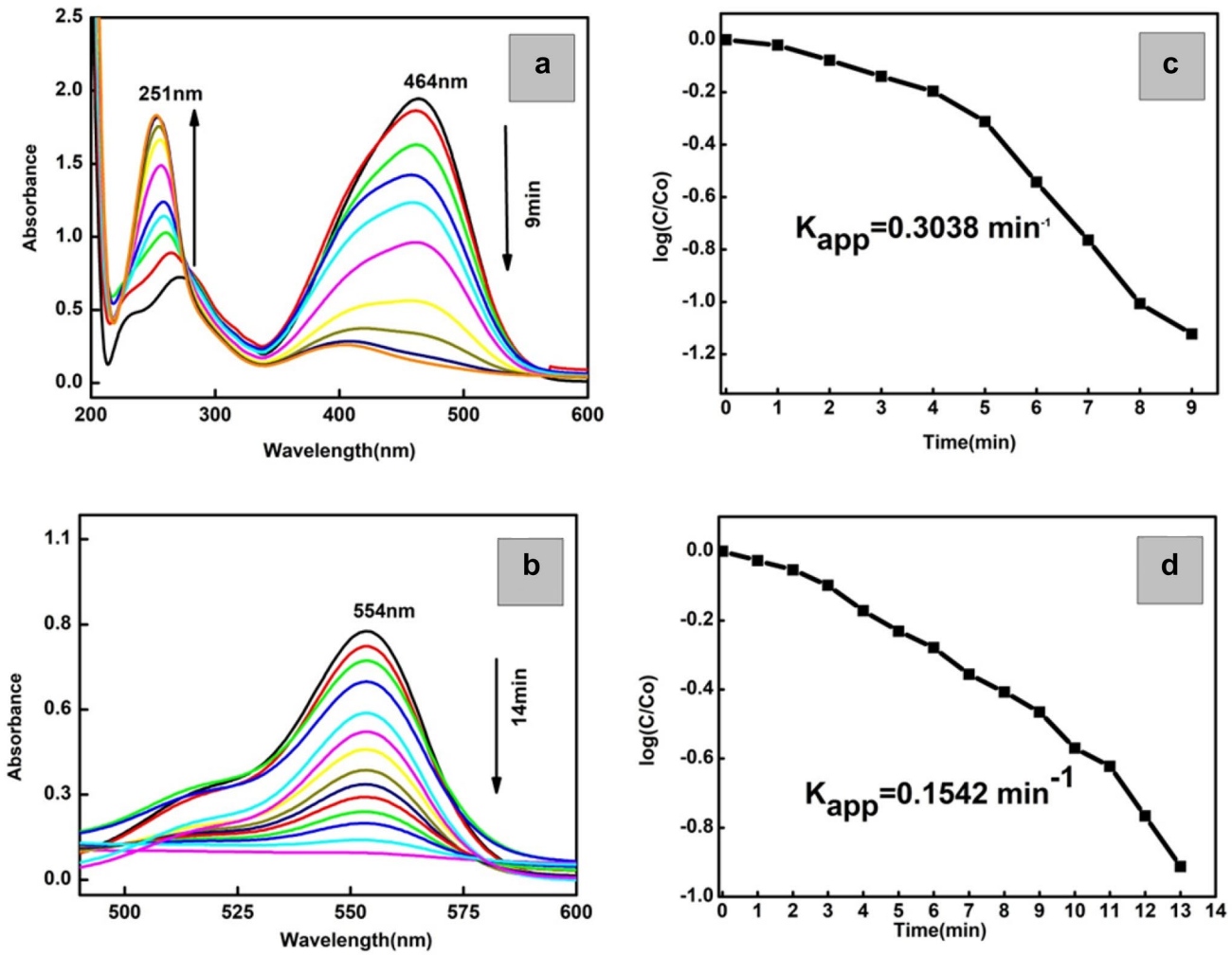

Fig. 11 Successive UV–Vis. Absorption spectra for the $NaBH_4$ reduction of MO and RhB catalyzed by AgNPs at 28 °C (picture **a** and **b** respectively) and plot of $log(C/C_0)$ against time 't' (picture '**c**' and '**d**' for MO and RhB respectively)

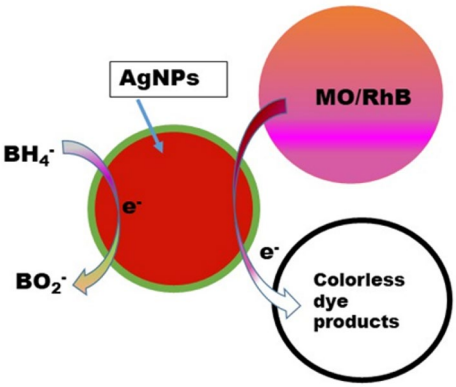

Fig. 12 A proposed scheme for reduction of MO/RhB by $NaBH_4$ in the presence of AgNPs

respectively. The pseudo-first-order rate constant for the reaction determined by plotting $\log(C/C_0)$ against time 't', are presented in Fig. 11 (picture 'c' and 'd' for MO and RhB respectively). The apparent rate constant K_{app} was calculated by assuming pseudo first order condition was found to be 0.3038 min^{-1} and 0.1542 min^{-1} for MO and RhB respectively.

As proposed by previous literature, the conversion of RhB and MO to their colorless reduced form involves the fast transfer of the electron from donor borohydride to the acceptor dye molecules assisted by added AgNPs [4, 24, 43]. No significant decrease in the intensity of absorption maxima of MO/RhB was observed in the solution containing MO/RhB and $NaBH_4$ even after 20 min in the absence of AgNPs, as the reductive degradation of MO/RhB was slow. On adding synthesized AgNPs to the above solution, the color of the solution decreases much faster indicating enhanced degradation process. The BH_4^- and MO/RhB molecules possibly get adsorbed on the surface of AgNPs without affecting their activity. The AgNPs surface will be refreshed and active throughout the reduction process as the surface of AgNPs are well passivated by Clammy cherry derived biomolecules keeping the AgNPs well dispersed and thus providing a large surface for the adsorption of the reactants. The adsorption of nucleophilic BH_4^- ions and electrophilic dye molecule over the AgNPs alters its standard electrode potentials to facilitate faster electron transport, where the AgNPs acts as a redox center and transport electrons from BH_4^- to MO/RhB. Figure 12 represents the proposed scheme of the AgNPs catalyzed the reduction of MO/RhB.

Table 2 evaluates the catalytic performance of the prepared AgNPs related to that of metal-based catalytic systems reported earlier.

It is evident from the comparison that the clammy cherry stabilized AgNPs has competing catalytic efficacy towards the reduction reaction. The good catalytic activity is being attributed to the better stabilization, and small size of the AgNPs synthesized by Clammy cherry mediated reduction. Therefore, clammy cherry protected stable AgNPs based catalytic systems can be conveniently used for the effective removal of dye pollutants in the water bodies.

Table 2 Comparison of catalytic activity of the synthesized AgNPs towards the reduction of MO and RhB with reported catalytic systems

Dye	System	Rate constant (min^{-1})	References
Methyl orange (MO)	Ag–Zeolite X	0.305	[44]
	AgNPs	0.0186	[45]
	PdAu/Dens-OH	0.0948	[46]
	Pt NPs	0.0029	[47]
	AuNPs	0.0049	[47]
	AgNPs	0.5853	[47]
	ZnO/carbon black-cellulose acetate	0.09	[48]
	$Au/CeO_2–TiO_2$	0.433	[49]
	Fe–Chitosan	0.1698	[50]
	Fe_3O_4–PPy–MMA/Ag	0.312	[51]
	Co-DNB	0.091	[52]
	RGO-Co-DNB	0.2912	[52]
	Ag–HNT	0.222	[53]
	AgNPs	0.3038	This work
Rhodamine blue (RhB)	Au NPs	0.453	[54]
	rGO–SiW	0.127	[55]
	AgNPs	0.600	[56]
	CuOS	0.036	[57]
	$Ag–Fe_2O_3–SiO_2$	0.152	[58]
	$Au/CeO_2–TiO_2$	0.222	[49]
	Au–PVP	0.033	[59]
	Ag–PVP	0.007	[59]
	Pt–PVP	0.305	[59]
	Fe–Chitosan	0.3804	[50]
	Co-DNB	0.108	[52]
	RGO-Co-DNB	0.3367	[52]
	$Ag–Fe_3O_4$	0.42	[60]
	AgNPs	0.1542	This work

4 Conclusion

Here, the green synthesis of AgNPs by reduction of silver ions using clammy cherry extract under microwave irradiation is reported for the first time. The synthesis of AgNPs was comparatively faster and prepared AgNPs colloid was

exceptionally stable for a considerably longer period of time. The formation AgNPs of the average size of 7.13 nm and narrow size distribution established that the polyfunctional molecules present in the clammy cherry extract are effective for reduction and proper stabilization of AgNPs. The clammy cherry reduced AgNPs exhibited excellent antibacterial activity, high catalytic efficacy, and better electrochemical response. It is concluded that the present study is highly promising as it could demonstrate a simple and fast synthesis method for the size and shape controlled AgNPs, having unique characteristics for biological, catalytic and sensing applications.

Acknowledgements The authors would like to thank the financial assistance to Femina K.S. Granted by University Grants Commission (under Faculty Development Program: Grant No. FIP/12th Plan/KLMG 009 TF 12 dated 20/04/2017), Government of India. The authors would like to thank SAIF STIC and Biotechnology Department of CUSAT, and Kerala, India for characterization facilities. The authors thank Dr. Bindu Sarmila and Dr. Neena George, Maharajas College, Ernakulam, Kerala, India for their valuable suggestions during the manuscript writing.

Compliance with ethical standards

Conflict of interest The authors declare that they have no conflict of interest.

References

1. Yan Y, Wang T, Li X et al (2017) Noble metal-based materials in high-performance supercapacitors. Inorg Chem Front 4:33–51
2. Francis S, Joseph S, Koshy EP, Mathew B (2017) Synthesis and characterization of multifunctional gold and silver nanoparticles using leaf extract of: *Naregamia alata* and their applications in the catalysis and control of mastitis. New J Chem 41:14288–14298
3. Tian K, Prestgard M, Tiwari A (2014) A review of recent advances in nonenzymatic glucose sensors. Mater Sci Eng C 41:100–118
4. Francis S, Joseph S, Koshy EP, Mathew B (2018) Microwave assisted green synthesis of silver nanoparticles using leaf extract of *Elephantopus scaber* and its environmental and biological applications. Artif Cells Nanomed Biotechnol 46:795–804
5. Wacławek S, Gončuková Z, Adach K et al (2018) Green synthesis of gold nanoparticles using *Artemisia dracunculus* extract: control of the shape and size by varying synthesis conditions. Environ Sci Pollut Res 25:24210–24219
6. Ganapuram BR, Alle M, Dadigala R et al (2015) Catalytic reduction of methylene blue and Congo red dyes using green synthesized gold nanoparticles capped by salmalia malabarica gum. Int Nano Lett 5:215–222
7. Murphy CJ, Sau TK, Gole AM et al (2005) Anisotropic metal nanoparticles: synthesis, assembly, and optical applications. J Phys Chem 13857–13870
8. Kumar THV, Sundramoorthy AK (2018) Non-enzymatic electrochemical detection of urea on silver nanoparticles anchored nitrogen-doped single-walled carbon nanotube modified electrode. J Electrochem Soc 165:B3006–B3016
9. Jodat A, Jodat A (2014) Photocatalytic degradation of chloramphenicol and tartrazine using Ag/TiO_2 nanoparticles. Desalin Water Treat 52:2668–2677
10. Wang M, Tian D, Tian P, Yuan L (2013) Synthesis of micron-SiO_2@nano-Ag particles and their catalytic performance in 4-nitrophenol reduction. Appl Surf Sci 283:389–395
11. Kandula V, Nagababu U, Behera M et al (2018) A facile green synthesis of silver nanoparticles: an investigation on catalytic hydroxylation studies for efficient conversion of aryl boronic acids to phenol. J Saudi Chem Soc 23:711–717
12. Vidhu VK, Aromal SA, Philip D (2011) Spectrochimica acta part A: molecular and biomolecular spectroscopy green synthesis of silver nanoparticles using *Macrotyloma uniflorum*. Spectrochim Acta Part A Mol Biomol Spectrosc 83:392–397
13. Francis S, Joseph S, Koshy EP, Mathew B (2017) Green synthesis and characterization of gold and silver nanoparticles using *Mussaenda glabrata* leaf extract and their environmental applications to dye degradation. Environ Sci Pollut Res 24:17347–17357
14. Kalantari K, Afifi ABM, Bayat S et al (2016) Heterogeneous catalysis in 4-nitrophenol degradation and antioxidant activities of silver nanoparticles embedded in Tapioca starch. Arab J Chem. https://doi.org/10.1016/j.arabic.2016.12.018
15. Schmitz BK, Euler WB, Taylor P et al (2013) Catalytic oxidation of indigo carmine in the presence of silver nanoparticles: application to groundwater analysis. Arab J Chem 6:195–198
16. Nanaei M, Nasseri MA, Allahresani A, Kazemnejadi M (2019) *Phoenix dactylifera* L. extract: antioxidant activity and its application for green biosynthesis of Ag nanoparticles as a recyclable nanocatalyst for 4-nitrophenol reduction. SN Appl Sci 1:1–12
17. Kaur J, Singh J, Rawat M (2019) An efficient and blistering reduction of 4-nitrophenol by green synthesized silver nanoparticles. SN Appl Sci 1:1060–1065
18. Sivaramakrishnan M, Jagadeesan Sharavanan V, Karaiyagowder Govindarajan D et al (2019) Green synthesized silver nanoparticles using aqueous leaf extracts of *Leucas aspera* exhibits antimicrobial and catalytic dye degradation properties. SN Appl Sci 1:1–8
19. Vinay SP, Udayabhanu NG et al (2019) Enhanced photocatalysis, photoluminescence, and anti-bacterial activities of nanosize Ag: green synthesized via *Rauvolfia tetraphylla* (devil pepper). SN Appl Sci 1:1–14
20. Sharma G, Kumar A, Sharma S et al (2019) Novel development of nanoparticles to bimetallic nanoparticles and their composites: a review. J King Saud Univ Sci 31:257–269
21. Ding J, Zhang K, Wei G, Su Z (2015) Fabrication of polypyrrole nanoplates decorated with silver and gold nanoparticles for sensor applications. RSC Adv 5:69745–69752
22. Luo X, Morrin A, Killard AJ, Smyth MR (2006) Application of nanoparticles in electrochemical sensors and biosensors. Electroanalysis 18:319–326
23. Yuan C, Xu Y, Zhong L et al (2013) Heterogeneous silver-polyaniline nanocomposites with tunable morphology and controllable catalytic properties. Nanotechnology 24:185602–185612
24. Suchomel P, Kvitek L, Prucek R et al (2018) Simple size-controlled synthesis of Au nanoparticles and their size-dependent catalytic activity. Sci Rep 8:1–11
25. Latha D, Prabu P, Gnanamoorthy G et al (2019) Size-dependent catalytic property of gold nanoparticle mediated by *Justicia adhatoda* leaf extract. SN Appl Sci 1:1–14
26. Lara HH, Ayala-Nuñez NV, Ixtepan-Turrent L, Rodriguez-Padilla C (2010) Mode of antiviral action of silver nanoparticles against HIV-1. J Nanobiotechnol 8:1–10
27. Samari F, Salehipoor H, Eftekhar E, Yousefinejad S (2018) Low-temperature biosynthesis of silver nanoparticles using mango leaf extract: catalytic effect, antioxidant properties, anticancer activity and application for colorimetric sensing. New J Chem 42:15905–15916

28. Syafiuddin A, Salmiati SM et al (2017) A review of silver nanoparticles: research trends, global consumption, synthesis, properties, and future challenges. J Chin Chem Soc 64:732–756
29. Sharma VK, Yngard RA, Lin Y (2009) Silver nanoparticles: green synthesis and their antimicrobial activities. Adv Colloid Interface Sci 145:83–96
30. Reddy GS, Saritha KV, Reddy YM, Reddy NV (2019) Eco-friendly synthesis and evaluation of biological activity of silver nanoparticles from leaf extract of *Indigofera barberi* Gamble: an endemic plant of Seshachalam Biosphere Reserve. SN Appl Sci 1:968
31. Ananda AP, Krishnamurthy NB, Savitha KR, Nagendra BS (2019) Biogenic synthesis of silver nanoparticles using *Priva cordifolia* leaf extract (PC@AgNPs) a potent antioxidant, antibacterial and catalytic activity. SN Appl Sci 1:1–13
32. Palai PK, Mondal A, Chakraborti CK et al (2019) Green synthesized amino-PEGylated silver decorated graphene nanoplatform as a tumor-targeted controlled drug delivery system. SN Appl Sci 1:1–18
33. Ramar K, Gnanamoorthy G, Mukundan D et al (2019) Environmental and antimicrobial properties of silver nanoparticles synthesized using *Azadirachta indica* Juss leaves extract. SN Appl Sci 1:1–11
34. Francis S, Joseph S, Koshy EP et al (2017) Microwave assisted green synthesis of silver nanoparticles using leaf extract of *Elephantopus scaber* and its environmental and biological applications. Artif Cells Nanomed Biotechnol 46:795–804
35. Guadie Assefa A, Adugna Mesfin A, Legesse Akele M et al (2017) Microwave-assisted green synthesis of gold nanoparticles using Olibanum gum (*Boswellia serrate*) and its catalytic reduction of 4-nitrophenol and hexacyanoferrate (iii) by sodium borohydride. J Clust Sci 28:917–935
36. Oza MJ, Kulkarni YA (2017) Traditional uses, phytochemistry and pharmacology of the medicinal species of the genus Cordia (Boraginaceae). J Pharm Pharmacol 69:755–789
37. Gupta R, Das Gupta G (2018) Isolation and characterization of flavonoid glycoside from *Cordia obliqua Willd*. leaf. Int J Green Pharm 12:73–79
38. Jain PK, Huang X, El-Sayed IH, El-Sayed MA (2007) Review of some interesting surface plasmon resonance-enhanced properties of noble metal nanoparticles and their applications to biosystems. Plasmonics 2:107–118
39. Mani U, Dhanasingh S, Arunachalam R et al (2013) A simple and green method for the synthesis of silver nanoparticles using ricinus communis leaf extract. Nanotechnology 2:59–63
40. Ibrahim HMM (2015) Science direct green synthesis and characterization of silver nanoparticles using banana peel extract and their antimicrobial activity against representative microorganisms. J Radiat Res Appl Sci 8:265–275
41. Latha M, Sumathi M, Manikandan R et al (2015) Biocatalytic and antibacterial visualization of green synthesized silver nanoparticles using *Hemidesmus indicus*. Microb Pathog 82:43–49
42. Panáček A, Kolář M, Večeřová R et al (2009) Antifungal activity of silver nanoparticles against Candida spp. Biomaterials 30:6333–6340
43. Naseem K, Farooqi ZH, Begum R, Irfan A (2018) Removal of Congo red dye from aqueous medium by its catalytic reduction using sodium borohydride in the presence of various inorganic nano-catalysts: a review. J Clean Prod 187:296–307
44. Zainal Abidin A, Abu Bakar NHH, Ng EP, Tan WL (2017) Rapid degradation of methyl orange by ag doped zeolite X in the presence of borohydride. J Taibah Univ Sci 11:1070–1079
45. Jyoti K, Singh A (2016) Green synthesis of nanostructured silver particles and their catalytic application in dye degradation. J Genet Eng Biotechnol 14:311–317
46. Ilunga AK, Khoza T, Tjabadi E, Meijboom R (2017) Effective catalytic reduction of methyl orange catalyzed by the encapsulated random alloy palladium–gold nanoparticles dendrimer. Chem Sel 2:9803–9809
47. Gupta N, Singh HP, Sharma RK (2011) Metal nanoparticles with high catalytic activity in degradation of methyl orange: an electron relay effect. J Mol Catal A Chem 335:248–252
48. Molla A, Sahu M, Hussain S (2016) Synthesis of tunable band gap semiconductor nickel sulphide nanoparticles: rapid and round the clock degradation of organic dyes. Sci Rep 6:1–11
49. Saikia P, Miah AT, Das PP (2017) Highly efficient catalytic reductive degradation of various organic dyes by Au/CeO_2–TiO_2nanohybrid. J Chem Sci 129:81–93
50. Ali F, Khan SB, Kamal T et al (2017) Chitosan coated cotton cloth supported zero-valent nanoparticles: simple but economically viable, efficient and easily retrievable catalysts. Sci Rep 7:1–16
51. Das R, Sypu VS, Paumo HK et al (2019) Silver decorated magnetic nanocomposite (Fe_3O_4@PPy-MAA/Ag) as highly active catalyst towards reduction of 4-nitrophenol and toxic organic dyes. Appl Catal B Environ 244:546–558
52. Sahoo PK, Thakur D, Bahadur D, Panigrahy B (2016) Highly efficient and simultaneous catalytic reduction of multiple dyes using recyclable RGO/Co dendritic nanocomposites as catalyst for wastewater treatment. RSC Adv 6:106723–106731
53. Akhondi M, Jamalizadeh E (2019) Fabrication of silver-modified Halloysite nanotubes and their catalytic performance in Rhodamine 6G and methyl orange reduction. Acta Chim Slov 66:136–144
54. Francis S, Koshy EP, Mathew B (2018) Microwave aided synthesis of silver and gold nanoparticles and their antioxidant, antimicrobial and catalytic potentials. J Nanostruct 8:55–66
55. Ucar A, Findik M, Gubbuk IH et al (2017) Catalytic degradation of organic dye using reduced graphene oxide e polyoxometalate nanocomposite. Mater Chem Phys 196:21–28
56. Vijayan R, Joseph S, Mathew B (2018) Green synthesis of silver nanoparticles using *Nervalia zeylanica* leaf extract and evaluation of their antioxidant, catalytic, and antimicrobial potentials. Part Sci Technol 3:1–11
57. Abay AK, Chen X, Kuo DH (2017) Highly efficient noble metal free copper nickel oxysulfide nanoparticles for catalytic reduction of 4-nitrophenol, methyl blue, and rhodamine-B organic pollutants. New J Chem 41:5628–5638
58. Li C, Sun J, Chen D et al (2016) Ag-decorated Fe_3O_4@SiO_2 nanorods: synthesis, characterization, and applications in degradation of dyes. J Nanomater 2016:1–8
59. Piella J, Merkoçi F, Genç A et al (2017) Probing the surface reactivity of nanocrystals by the catalytic degradation of organic dyes: the effect of size, surface chemistry and composition. J Mater Chem A 5:11917–11929
60. Ai L, Zeng C, Wang Q (2011) One-step solvothermal synthesis of Ag–Fe_3O_4 composite as a magnetically recyclable catalyst for reduction of Rhodamine B. Catal Commun 14:68–73